

# Influence of solidification rate and alloying elements on structure, mechanical and electrical properties of Al-Cu-X alloys

A. Kalkanoglu<sup>1</sup>, H. Kaya<sup>2\*</sup>, U. Büyük<sup>2</sup>, E. Çadırli<sup>3</sup>

<sup>1</sup>Siirt University, Education Faculty, Department of Science Education, Siirt, Turkey

<sup>2</sup>Erciyes University, Education Faculty, Department of Science Education, Kayseri, Turkey

<sup>3</sup>Niğde Ömer Halisdemir University, Faculty of Arts and Sciences, Department of Physics, Niğde, Turkey

Received 17 September 2021, received in revised form 1 October 2021, accepted 6 October 2021

## Abstract

The present work aims to explore the effects of the alloying elements (Si, Bi, Sb, Ni, and Co) and solidification rates ( $V$ ) on the microstructural morphology, microhardness, ultimate tensile strength and electrical resistivity of Al-Cu based eutectic alloys by Bridgman-type solidification apparatus, metallographic observation, scanning electron microscopy, microhardness testing, tensile testing and four-point probe testing. Firstly, the Al-33 Cu-2X (wt.%) samples were produced by using metals of high purity ( $> 99.95\%$ ) in the vacuum and hot-filling furnaces; these alloys were unidirectionally solidified under different solidification rates,  $V$  ( $8.28\text{--}167.08\ \mu\text{m s}^{-1}$ ) and constant temperature gradient,  $G$  (average  $8.50\ \text{K mm}^{-1}$ ). Secondly, metallographic examination and measurement processes: lamellar spacings ( $\lambda$ ), microhardness (HV), ultimate tensile strength (UTS) and electrical resistivity ( $\rho$ ) were measured and expressed as functions of  $V$ . It has been found that the addition of the alloying elements (AE) content in Al-Cu eutectic as well as increasing of  $V$  lead to a decrease of lamellar spacings. On the contrary, the values of HV, UTS, and  $\rho$  increase with increasing  $V$  values and the addition of alloying elements. Relationships between  $\lambda$ - $V$ ,  $\lambda$ -HV,  $\lambda$ -UTS ( $\sigma$ ) and  $\lambda$ - $\rho$  were found by regression analysis, and the results found in this research were compared with the previous similar studies.

Key words: Al-Cu alloys, alloying, lamellar spacings, microhardness, ultimate tensile strength, electrical resistivity

## 1. Introduction

Aluminum is the third most common element in the earth's crust and is classified as a light metal. Its strength can be increased by alloying, mechanical and heat treatment, thereby improving its mechanical properties [1]. Copper is a strong precipitation reinforcement element in aluminum alloys. Among the aluminum alloys, wrought Al-Cu (2xxx), Al-Mg-Si (6xxx), and Al-Cu-Zn-Mg (7xxx) series alloys have been extensively studied due to their high specific strength [2]. Al-Cu alloys have been under active scientific research and technological development for more than 100 years because of their applications in lightweight constructions [3]. Nowadays, Al-Cu alloys are extensively used in numerous engineering applications such as aerospace, rocket, vehicles, electronic,

and building industries due to their low density, light weight, good oxidation resistance, reasonable ductility, and superior mechanical properties [1, 4].

Researchers have focused on improving the mechanical and electrical properties of aluminum alloys for use in a broader range of applications. The mechanical and electrical properties of aluminum alloys can be improved by different methods such as cold working, heat treatment, and adding alloying elements to the aluminum matrix. The addition of alloying elements (AE) and microstructure impurities can control the required strength and electrical conductivity of the alloy. In other words, the addition of grain refiners creates a large number of nuclei in the melt, thereby inducing the formation of small equiaxed grains of  $\alpha$ -Al. Grain refining leads to the even distribution of second phase components and the formation of micropores

\*Corresponding author: tel.: +90-352-206 77 77; e-mail address: [hasankaya@ercives.edu.tr](mailto:hasankaya@ercives.edu.tr)

in the casting structure, which improves mechanical properties and machinability and also changes electrical properties [5–7].

When the studies conducted in the last decade are examined, while some studies are available regarding the effect of mechanical properties of Al-Cu alloys produced by AE such as Co, Sn, Zn, Zr, Ti, Mg, Mn, Sc, etc. [8–13] where the amount of AE is generally higher than 0.5 wt.% (macro additions), the same reach is a trend to obtain aluminum alloys with a better combination of properties by micro-alloying the existing commercial alloys, i.e., by addition of trace amounts (< 0.1 wt.%) of elements like Ag, Sn, Zr, Cd, In, Ti, Sc, etc. Trace addition of these alloying elements influences the microstructure and mechanical properties of the base alloy [14–17].

The addition of 0.3 Mg and 0.05 Ti (wt.%) has been found to increase the strength of Al-4.5Cu alloy by about 10% [18]. Experimental results show that even small variations in 0.1 Sn (0–0.1 wt.%) content result in significant changes in structure and mechanical properties of 2219 alloy [19]. These studies show that the strength increases with an increase in Sn concentration in the alloy up to 0.06 wt.%. Similarly, Salihu et al. [20] investigated the effect of adding Mg on the mechanical properties and structure of Al-Cu alloys. They reported that the increase in Mg percentage leads to an increase in hardness and tensile strength for the studied alloys, the addition of 2.5 wt.% Mg can improve hardness by 23%, while tensile strength can be improved by 70%.

Another physical property of materials is electrical resistivity. Electrical resistivity ( $\rho$ ) is the most important parameter of conducting metallic materials used in electrical engineering. Electrical resistivity is very sensitive to the microstructure of the metallic materials owing to disturbances in the atomic crystal structure, solute atoms and crystal defects [21]. However, the electrical conductivity of commercially pure aluminum is higher than all aluminum materials and alloys. It has limited application due to its very low mechanical strength and toughness [22]. The demand for high strength and electrically conductive aluminum alloys has increased for cable applications and transmission lines. Practically, the strength of aluminum can be significantly improved by adding AE to pure aluminum. However, on the other hand, a considerable reduction in electrical conductivity occurs due to the solute atoms and impurities formed by substituting alloying elements. Therefore, it is a major challenge to play with the strength of pure aluminum such that the reduction in electrical conductivity is still acceptable and valid for the chosen application. The electrical conductivity of metals is affected by the structure of the material, as it is susceptible to electron scattering disruption due to a defect in the crystal structure or solute. Hagemaijer [23] reported that the

relationship between electrical conductivity and mechanical properties was found to be "C-shaped" for most heat-hardened aluminum alloys. Accordingly, recent research has focused on developing high strength Al alloys with high electrical properties through novel processing and production techniques [24]. The improved properties can be obtained by different methods such as adding alloying elements, heat treatment and cold working of the Al matrix. The addition of alloying elements, including microelements, macroelements, and microstructures, can control the required strength and electrical properties of the alloy [25].

The mechanical properties of unidirectionally solidified Al-Cu based alloys, which are essential commercial materials, have been reported in different researches [4, 8–20]. The solidification parameters (e.g., temperature gradient and solidification rate) and the addition of the AE directly affect the microstructural formation of the alloys. Thus, the microstructures play a crucial role in the physical properties (mechanical and electrical) of metallic alloys. The effects of applied solidification parameters on physical properties have been studied intensively [8, 10, 12, 15, 26–36]. Experimental researches show that the solidification condition and AE strengthen the alloy through refined grains and improve the mechanical properties. However, the effects of solidification condition and AE on the microstructure, mechanical properties (microhardness and ultimate tensile strength), and electrical properties of the Al-Cu-X alloys have been worth to be investigated systematically. For this purpose, the dependences of microstructure ( $\lambda$ ), microhardness (HV), ultimate tensile strength (UTS), and electrical resistivity ( $\rho$ ) on the solidification rate ( $V$ ) and AE for directionally solidified Al-33Cu-2X (wt.%) alloys were investigated.

## 2. Materials and methods

### 2.1. Material preparation

In this study, Al, Cu, Si, Bi, Sb, Ni, and Co metals with purities greater than 99.95% were used. Al-Cu-X molten alloys were prepared in a vacuum melting furnace with nominal 33 wt.% copper and 2 wt.% alloying elements (Si, Bi, Sb, Ni, and Co). AE were introduced in the form of Al-33%Cu master alloy. The melt was degassed for about 20 min to ensure homogeneous mixing of the additions. Then, the molten alloy was poured into graphite crucibles with dimensions of 200 mm in height, 4 mm in diameter and volume of  $2.5 \times 10^3 \text{ mm}^3$  held in a hot-filling furnace at about 100 K above the melting temperature of the alloy. The molten alloy in the graphite crucible was unidirectionally solidified to obtain an utterly full sample. After that, each sample was positioned in a vertical-type

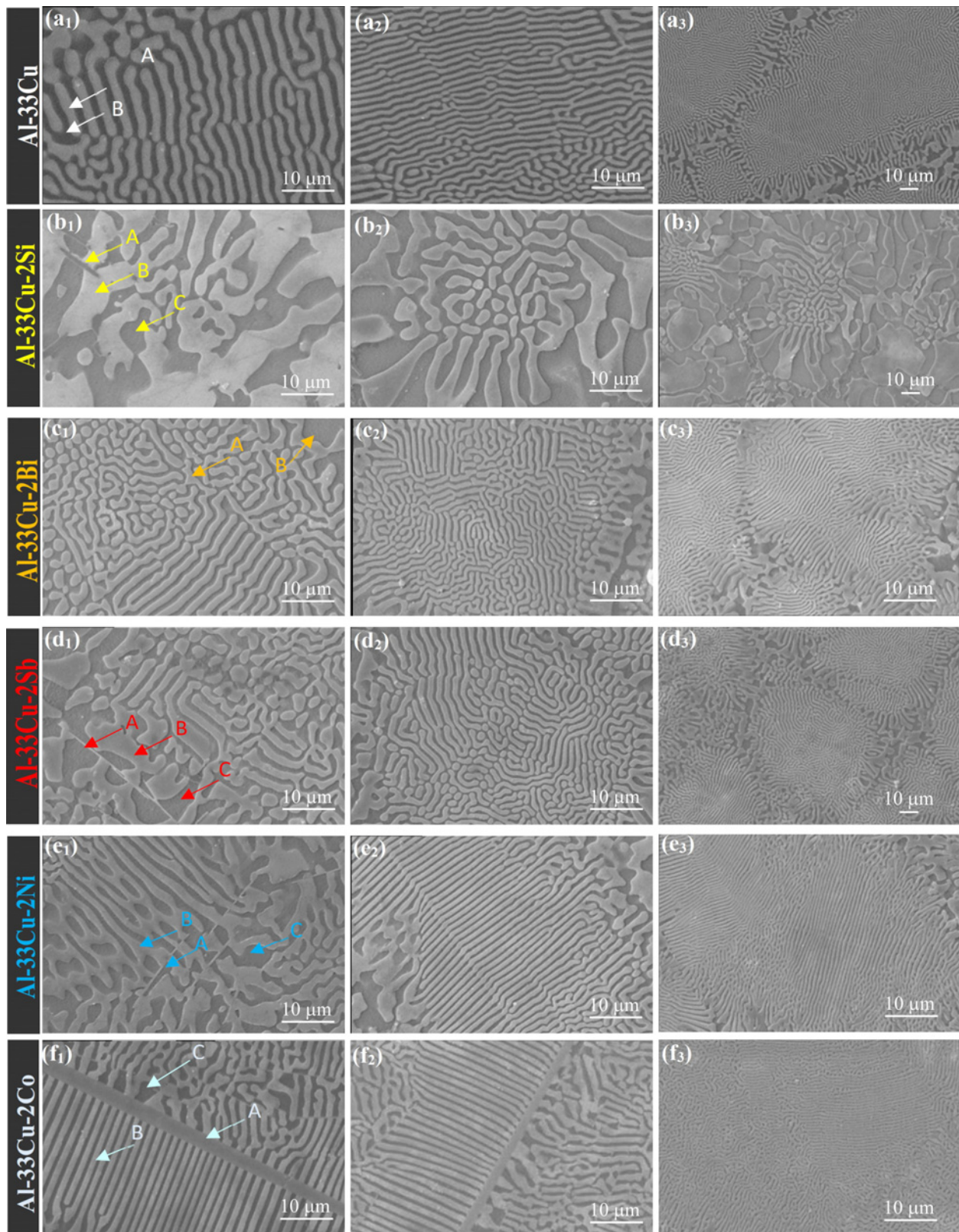


Fig. 1. The solidification morphologies of the Al-Cu-X for the different solidification rates: (a1-b1-c1-d1-e1-f1)  $V \cong 8.28 \mu\text{m s}^{-1}$ , (a2-b2-c2-d2-e2-f2)  $V \cong 41.60 \mu\text{m s}^{-1}$ , and (a3-b3-c3-d3-e3-f3)  $V \cong 167.08 \mu\text{m s}^{-1}$ .

Bridgman furnace within a graphite cylinder (made to protect the sample). After stabilizing the thermal

conditions, the samples were grown at a constant  $G$  ( $8.50 \text{ K mm}^{-1}$ ) with different  $V$  from  $8.28 \mu\text{m s}^{-1}$  to

$167.08 \mu\text{m s}^{-1}$  (for each alloy) by using different speed synchronous motors (1, 2, 5, 10, and 20 rpm). The details of the experimental procedure are given in the previous works [26, 27].

## 2.2. Measurement of temperature gradient ( $G$ ), solidification rate ( $V$ ), and lamellar spacings ( $\lambda$ )

The temperature in the sample was measured with three K-type thermocouples (0.25 mm diameter and insulated) placed with a distance ( $\Delta X$ ) of 10 mm. All thermocouples were inserted into alumina tubes (to be protected from the melt), and the ends of the thermocouples were connected to a computer and a data logger. The temperatures in the sample were recorded continuously by the computer. The temperature difference between two consecutive thermocouples ( $\Delta T$ ) was read from the data logger when the solid-liquid interface was at the second thermocouple. The temperature gradient ( $G$ ) was calculated by  $\Delta T$  and  $\Delta X$  ( $G = \Delta T / \Delta X$ ). When the solid-liquid interface comes from the 1st to the 2nd thermocouple, the elapsed time ( $\Delta t$ ) is read from a computer.

After the solidification stage, sanding and polishing processes were carried out on the samples to reveal the microstructures. For this purpose, the solidified sample was extracted from the crucible, and 2 cm in length from the top and bottom were cropped off and discarded. The transverse and longitudinal sections of the samples were sanded with several SiC papers and polished by 6, 3, 1, and  $0.25 \mu\text{m}$  diamond pastes. Finally, the polished samples were etched with Keller's microetchant (20 ml distilled  $\text{H}_2\text{O}$  + 20 ml  $\text{HNO}_3$  + 20 ml  $\text{HCl}$  + 5 ml  $\text{HF}$ ) for 5 s for Si added, modified Murakami's reagent (100 ml of  $\text{H}_2\text{O}$ , 10 g of  $\text{NaOH}$  and 10 g of  $\text{C}_6\text{N}_6\text{FeK}_3$ ) for 5–10 s for Co added, 10 vol.%  $\text{HF}$  + 90 vol.%  $\text{H}_2\text{O}$  for 5–10 s Sb added, and 12 %  $\text{HF}$  in  $\text{H}_2\text{O}$  enchant for 8–10 s for Ni and Bi added to Al-Cu eutectic. After the metallographic process, the microstructures of the samples were revealed. Some typical SEM images of solidification morphologies of Al-Cu-X samples are shown in Fig. 1.

The lamellar spacings ( $\lambda$ ) were measured from the SEM photos of solidification structures taken from both longitudinal and transverse sections of the specimens with the intersection method [26] and obtained the average  $\lambda$  values for each sample (Fig. 2). 15–20 measurements were made from different regions of each sample to increase statistical reliability.

## 2.3. Mechanical tests (HV and UTS)

One of the components of this research is focused on the effect of the alloying elements (AE) as well as solidification rate ( $V$ ) on mechanical properties (HV and UTS) and also obtain the relationships between

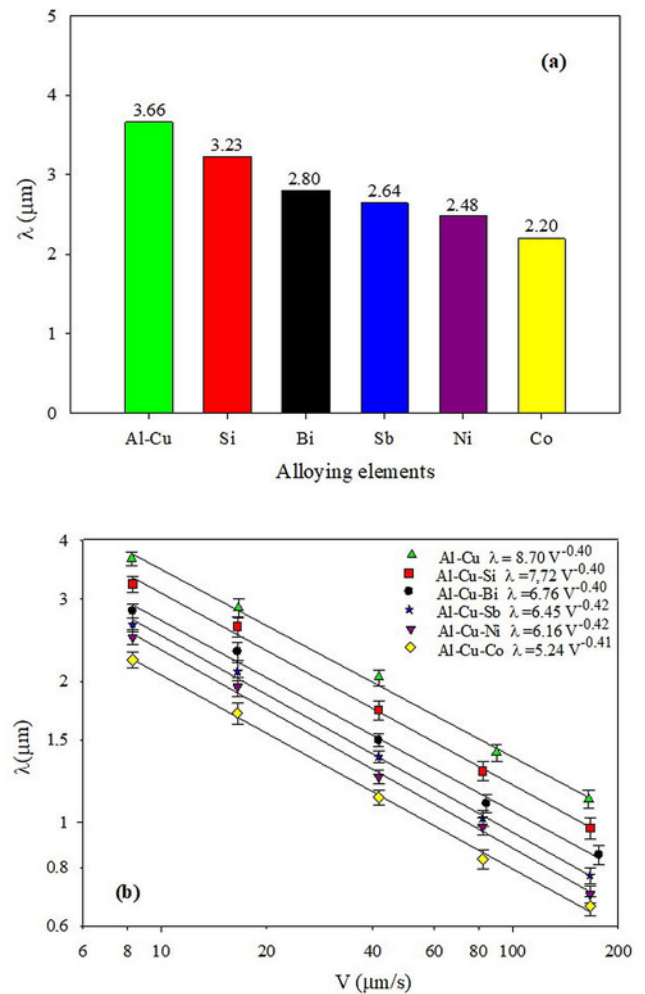


Fig. 2. (a) Variation of lamellar spacings vs. alloying elements and (b) variation of lamellar spacings vs. solidification rate.

them for Al-Cu-X alloys. Microhardness values of the samples were measured using a *DuraScan* digital hardness test device with the ability to apply a load from 1 g to 10 kg. In this work, 100 g load was applied to the sample for 10 seconds. HV values were measured on a transverse section of the samples in about 10 different regions. After that, average microhardness values were found for each sample. Measured values of HV are given in Fig. 3.

The tensile tests were made at room temperature at a strain rate of  $10^{-3} \text{s}^{-1}$  with a Shimadzu AG-XD universal testing machine according to ASTM-E8-04 [37]. The round rod tensile samples with a diameter of 4 mm and a gauge length of 40 mm were prepared from the directionally solidified alloy system. The pull direction was chosen parallel to the growth direction of the samples. The tensile measurements were repeated four times, and the average value was taken. The measured UTS values are presented in Fig. 4.

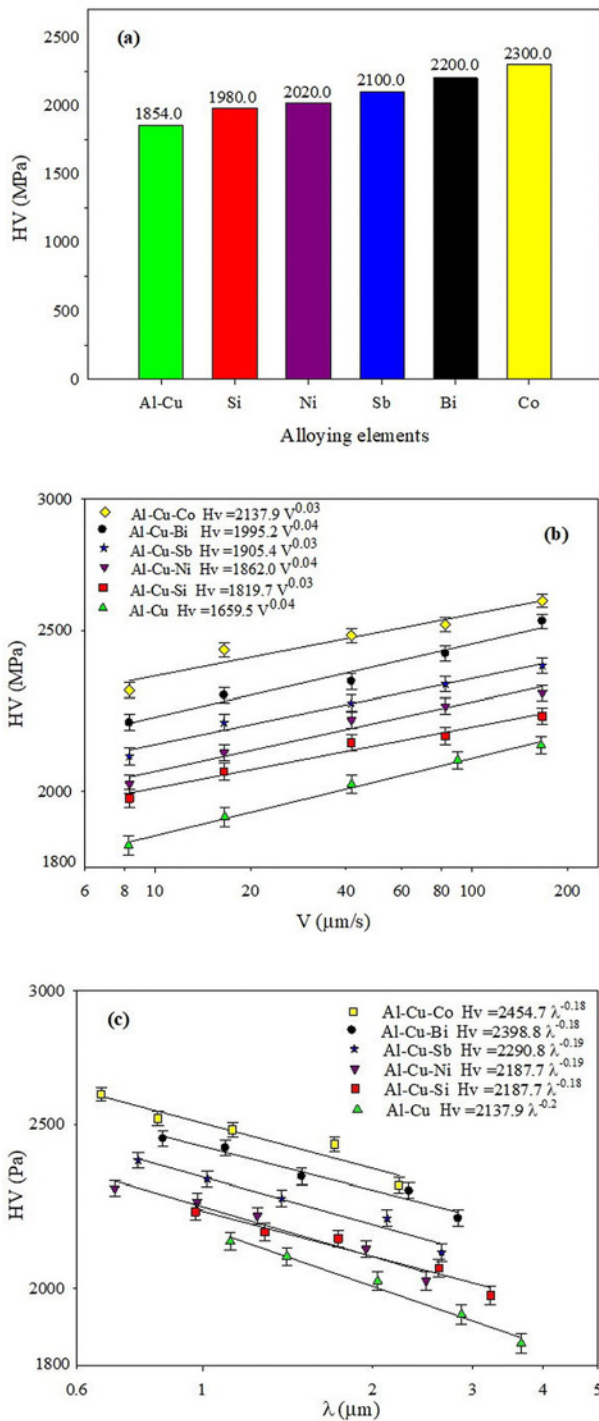


Fig. 3. (a) Variation of microhardness vs. alloying elements, (b) variation of microhardness vs. solidification rate, and (c) variation of microhardness vs. lamellar spacings.

#### 2.4. Measurement of electrical resistivity

Another component of this research was to investigate the relationships among the alloying elements, solidification rate and electrical resistivity. For this

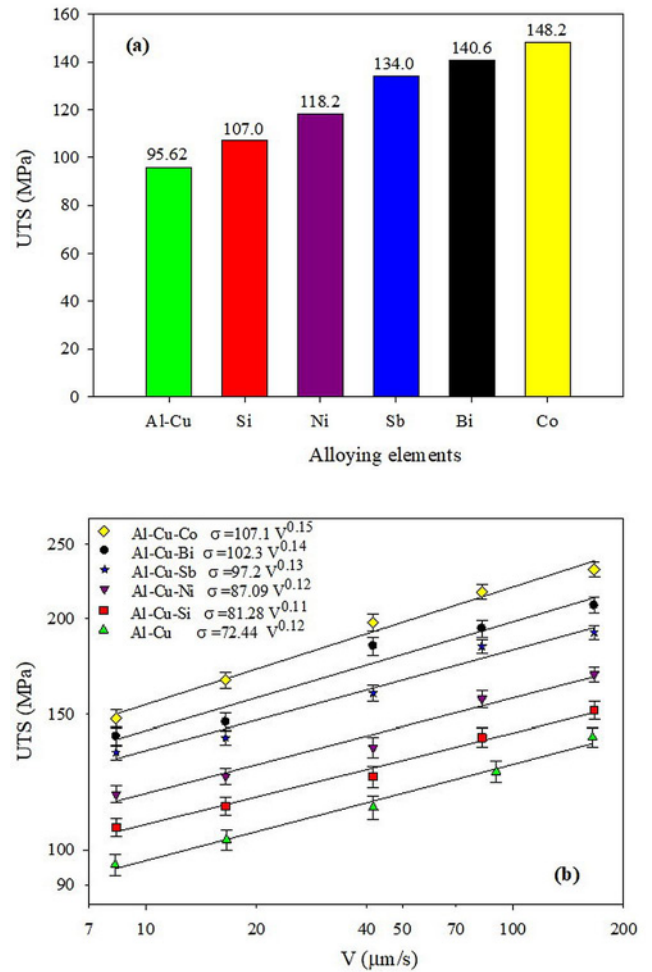


Fig. 4. (a) Variation of UTS vs. alloying elements and (b) variation of UTS vs. solidification rate.

purpose, the electrical resistivity ( $\rho$ ) measurements of the Al-Cu-X alloys were made using the standard d.c. four-point probe method at room temperature. In this method, the effects of contact resistance between the sample and electrical contacts can be eliminated and therefore it is most suitable for low and accurate resistivity measurements [38]. The d.c. four-point probe method has proven to be a convenient tool for electrical resistivity measurements. The electrical resistivity measurements were made by four platinum wire probes contacts to the surface of a cleaned sample. A Keithley-2400 model source meter was used to provide constant current, and the potential drop was measured with a Keithley-2700 model multimeter connected to a computer. The measured  $\rho$  values are given in Fig. 5.

### 3. Results and discussion

#### 3.1. Microstructural characterization

The microstructures and analysis of the chemi-

Table 1. The chemical composition analysis of the Al-33Cu-2X (X = Si, Bi, Sb Ni, and Co) alloys

Figure	Composition	A (phase)	Elmt (wt.%)	B (phase)	Elmt (wt.%)	C (phase)	Elmt (wt.%)
Fig. 1a <sub>1</sub>	Al-33Cu	Al <sub>2</sub> Cu	Al: 71.30 Cu: 28.70	Al( $\alpha$ )	Al: 93.66 Cu: 6.44	–	–
Fig. 1b <sub>1</sub>	Al-33Cu-2Si	Si	Al: 43.98 Cu: 5.87 Si: 50.15	Al <sub>2</sub> Cu	Al: 45.59 Cu: 53.68 Si: 0.73	Al( $\alpha$ )	Al: 94.20 Cu: 4.90 Si: 0.90
Fig. 1c <sub>1</sub>	Al-33Cu-2Bi	Al <sub>2</sub> Cu	Al: 51.60 Cu: 48.40	Al( $\alpha$ )	Al: 88.56 Cu: 10.85 Bi: 0.59	–	–
Fig. 1d <sub>1</sub>	Al-33Cu-2Sb	AlSb	Al: 84.07 Cu: 14.37 Sb: 1.56	Al <sub>2</sub> Cu	Al: 46.35 Cu: 53.50 Sb: 0.15	Al( $\alpha$ )	Al: 92.74 Cu: 7.10 Sb: 0.16
Fig. 1e <sub>1</sub>	Al-33Cu-2Ni	Al <sub>3</sub> Ni	Al: 75.23 Cu: 22.76 Ni: 2.01	Al <sub>2</sub> Cu	Al: 50.40 Cu: 48.75 Ni: 0.85	Al( $\alpha$ )	Al: 71.87 Cu: 27.66 Ni: 0.47
Fig. 1f <sub>1</sub>	Al-33Cu-2Co	Al <sub>7</sub> CoCu <sub>2</sub>	Al: 47.77 Cu: 38.32 Co: 13.91	Al <sub>2</sub> Cu	Al: 47.63 Cu: 52.37	Al( $\alpha$ )	Al: 90.57 Cu: 9.43

cal composition of Al-Cu-X samples were analyzed by SEM with an Energy Dispersive X-ray spectrometer (EDX) and an image analyzer. Typical photographs taken from SEM for different AE and  $V$  are shown in Fig. 1. Additionally, to designate and make sure of solid phases, analysis of composition in solid phases of the sample was made by Energy-Dispersive X-ray spectroscopy (EDX) at 20 keV with the X-ray lines. The details of quantitative chemical composition analyses for AE are given in Fig. 1 and Table 1. In the Al-Cu eutectic, it is seen that the matrix Al and white lamellar Al<sub>2</sub>Cu intermetallic phases (IMC) have a regular arrangement of microstructure (Fig. 1a). As a result of analyses, in Co and Sb addition (Fig. 1d), Al<sub>2</sub>Cu white lamellar IMC phase and AlSb IMC rod phase were observed on the main phase of Al ( $\alpha$ ). The results of composition analysis details are presented in Table 1. In Ni addition, Al<sub>2</sub>Cu white lamellar IMC phase and Al<sub>3</sub>Ni IMC rod phase were observed on the main phase of Al ( $\alpha$ ) (Fig. 1e). Furthermore, it was observed that three different phases were grown on the Al ( $\alpha$ ) main phase, namely the Al<sub>2</sub>Cu white lamellar IMC and the thick rod Al<sub>7</sub>CoCu<sub>2</sub> IMC phase (Fig. 1f and Table 1).

Figure 1 shows series of SEM micrographs showing the microstructure of various Al-Cu based eutectic alloy, with pure Si, Bi, Sb, Ni, and Co as the control. The microstructures of Al-Cu-X multicomponent alloys are similar to the Al-Cu eutectic alloy and generally consist of Cu lamellae that were regularly allocated in

solid  $\alpha$ -Al matrix phase. The microstructures of refinement copper lamellae have been distributed over an entire sample in between the area where Al( $\alpha$ )-grains are offered due to the AE. The solidification SEM microstructures show that refined lamellae have thickness and distribution differences for similar casting conditions. It is shown from Fig. 2a the lamellar spacings ( $\lambda$ ) decrease by the addition of AE to base Al-Cu eutectic. The values of  $\lambda$  are 3.66, 3.23, 2.83, 2.64, 2.48, and 2.22 in  $\mu\text{m}$  for Al-Cu eutectic and Al-Cu-X alloys containing Si, Bi, Sb, Ni, and Co, respectively, at the same solidification rate ( $V \cong 8.28 \mu\text{m s}^{-1}$ ). The smallest lamellar spacing, 0.66  $\mu\text{m}$ , was measured from the Al-Cu-Co sample with 167.08  $\mu\text{m s}^{-1}$  condition. The addition of AE led to a decrease in lamellar spacings by 11, 22, 27, 32, and 39% for Si, Bi, Sb, Ni, and Co added to Al-Cu eutectic, respectively, for  $V \cong 8.28 \mu\text{m s}^{-1}$ .

As is well known, low solidification conditions allow more intense atomic diffusion. In this way, the higher lamellar spacings are attributed to the more intense collaborative growth and the higher diffusion length. On the contrary, the smallest lamellar spacing was found at the highest  $V$  value. As mentioned before, Al-Cu-X alloys were unidirectionally solidified under different  $V$  and a constant  $G$ . As expected, while the values of  $V$  were increased, the lamellar spacings decreased. The regression analysis gives the proportionality equation as:

$$\lambda = k_1 \times V^a, \quad (1)$$

where  $k_1$  and  $a$  are a constant and an exponent value of  $V$ , respectively.

The values of  $a$  are equal to 0.40, 0.40, 0.40, 0.42, 0.42, and 0.41 for Al-Cu and Al-Cu-X alloys containing Si, Bi, Sb, Ni, and Co, respectively. The exponent values of  $V$  (0.40–0.42) are in good agreement with the range of exponent values (0.35–0.45) reported by different researchers [8, 26–29, 38] for similar alloys such as Al-Cu-Co [8], Al-12.6Si-2X alloys [26], Al-1.9Mn- $x$ Fe ( $x = 0.5, 1.5, \text{ and } 5 \text{ wt.}\%$ ) [28], Al-Cu-Mg [29], Ti-Al-Nb [36], Al-Cu-Ag [39], and under similar growth conditions. But, the exponent values for  $V$  are slightly lower than the value of 0.50 predicted by the Jackson and Hunt [40] theory for binary eutectic.

### 3.2. Influence of solidification rates and alloying elements on microhardness

To see the influence of alloying elements (AE) and solidification rate ( $V$ ) on microhardness (HV) of Al-Cu based alloys, a series of experiments were made. The microhardness measurements results are given in Fig. 3. Figure 3 shows the variation of HV depending on AE (Fig. 3a) and  $V$  (Fig. 3b). The results showed that the addition of all AE improved the HV of the Al-Cu eutectic. While the HV value of the Al-Cu eutectic was measured as 1854.8 MPa, the HV values of the Al-Cu-X alloys containing Si, Bi, Sb, Ni, and Co were measured as 1980, 2202, 2100, 2020, and 2300 MPa, respectively, for the same growth conditions. As shown from these values, the sample Al-Cu-Co has the highest microhardness value (2300 MPa). The addition of AE caused an increase in HV values about 6, 16, 12, 8, and 19 for Si, Bi, Sb, Ni, and Co added to Al-Cu, respectively, for  $V \cong 8.28 \mu\text{m s}^{-1}$ .

As mentioned before, after Al-Cu-X bulk samples solidified with different solidification rates, microhardness measurements were carried out. As seen in Fig. 3b, increasing the  $V$  values from 8.28 to  $167.08 \mu\text{m s}^{-1}$  increases HV values from 1854.8 MPa to 2604.2 MPa depending on  $V$  and AE. The linear regression analysis gives the proportionality equation as:

$$\text{HV} = k_2 \times V^b, \quad (2)$$

where  $k_2$  and  $b$  are a constant and an exponent value of  $V$ , respectively.

While the microhardness values of the Al-Cu eutectic increase from 1854.8 to 2131.9 MPa, the values of samples Al-Cu-Co increase from 2300 to 2604.2 MPa for the same solidification conditions. The exponent values of  $V$  were 0.04, 0.03, 0.04, 0.03, 0.04, and 0.03 for Al-Cu eutectic and Al-Cu-X alloys containing Si, Bi, Sb, Ni, and Co, respectively. These exponent val-

ues of  $V$  in this work are in good agreement with the values of 0.05, 0.03, 0.04, 0.05, and 0.07 found by Çadırılı et al. [8] for Al-Cu-Co eutectic, Kaygısız and Maraşlı [29] for Al-Cu-Mg, Büyük et al. [30] for Al-Cu-Si-Fe, Kaya et al. [31] for Al-Mn- $x$ Si, and Lapin and Marecek [32] for Ni-Al based alloys, respectively. But these exponent values are smaller than the 0.09 and 0.16 reported by Kaya and Aker [26] for Al-Si-X alloys and Fan et al. [33] for Al-Ti alloy. The differences may be due to the different alloy compositions, microstructural features, and experimental errors.

The variation of the microhardness as a function of the lamellar spacing is also given in Fig. 3c. As shown in Fig. 3c, it can be concluded that a decrease in the values of  $\lambda$  leads to an increase in the values of HV, and the relationship between the  $\lambda$  and HV can be expressed as:

$$\text{HV} = k_3 \times \lambda^{-c}, \quad (3)$$

where  $k_3$  and  $c$  are a constant and an exponent value of  $\lambda$ , respectively.

In the present work, the values of the exponent relating to the lamellar spacings were obtained to be: 0.20, 0.18, 0.18, 0.19, 0.19, and 0.18 for Al-Cu, Al-Cu-Si, Al-Cu-Bi, Al-Cu-Sb, Al-Cu-Ni and Al-Cu-Co, respectively. The exponent values of the lamellar spacings ( $\lambda$ ) obtained in the literature range from 0.15 to 0.50 for  $\lambda$  [8, 29, 32–36] for different alloy systems under similar solidification conditions. It can be observed that the exponent values of microstructure in this study are generally in agreement with some of the obtained values reported in the literature. Some differences among the exponent values might be due to different alloy compositions, different microstructures and experimental errors.

### 3.3. Dependence of ultimate tensile strength on alloying elements and solidification rates

The dependences of the UTS on alloying elements (AE) and the solidification rate ( $V$ ) in the range of  $8.28\text{--}167.08 \mu\text{m s}^{-1}$  were also investigated. For this objective, several UTS experiments were done, and results are presented in Fig. 4a. The addition of AE has different influence on the UTS, but the differences between low and high solidification rates all increased after alloying. Furthermore, the results showed that the addition of all AE improved the UTS of Al-Cu eutectic alloy. The addition of AE led to an increase in UTS values by 10 % for Si, 32 % for Bi, 29 % for Sb, 19 % for Ni, and 35 % for Co added to Al-Cu based alloy for  $V \cong 8.28 \mu\text{m s}^{-1}$  condition. As can be seen from these results, the tensile strength of the alloy containing Co is higher than the other added alloys. This situation can be explained by the presence of thick rod-

like  $\text{Al}_7\text{CoCu}_2$  IMC phases formed in the  $\alpha$ -Al matrix phase.

After the solidification and metallographic processes, UTS experiments were carried out from Al-Cu-X cylindrical metal alloy sample with a diameter of 4 mm. As seen from Fig. 4b, an increase in  $V$  leads to an increase in the UTS values ( $\sigma$ ). The dependence of UTS ( $\sigma$ ) on  $V$  can be expressed as:

$$\sigma = k_4 \times V^d, \quad (4)$$

where  $k_4$  and  $d$  are a constant and an exponent value of  $V$ , respectively.

The values of UTS increase with increasing the solidification rate (Fig. 4b). It was found that AE added to Al-Cu based alloy increased the  $V$  values from 8.28 to 167.08  $\mu\text{m s}^{-1}$ , the UTS values increased from 95.6 to 231.7 MPa. The Al-33Cu-2Co sample had the highest UTS and HV values because lamellar spacings were decreased, and copper grains were maximally refined. So, homogeneous distribution of copper particles all over the matrix phase ( $\alpha$ -Al) formed along the lamellar regions, improving the microhardness and UTS of the matrix phase. The  $c$  values were 0.12, 0.11, 0.15, 0.13, 0.12, and 0.15 for Al-Cu based alloy and Al-Cu-X alloys containing Si, Bi, Sb, Ni, and Co, respectively. The range of exponent values (0.11–0.15) in this study is in excellent agreement with the values ranging from 0.09 to 0.16 reported by Kaya and Aker [26] for Al-Si-X alloys, Kaygısız and Maraşlı[29] for Al-Cu-Mg, Kaya et al. [31] for Al-Mn- $x$ Si, Fan et al. [34], and Lapin et al. [35] for TiAl-based alloys. Differences in the exponent values may be owing to experimental errors, different microstructures, and compositions.

### 3.4. Dependence of electrical resistivity on alloying elements and solidification rates

To show the influence of alloying elements (AE) and solidification rates ( $V$ ) on electrical resistivity ( $\rho$ ) of Al-Cu alloys, a series of experiments were made. Resistivity measurements were made by the four-probe method at room temperature. The measured values of the electrical resistivity ( $\rho$ ) are given in Fig. 5. Figure 5a shows the change of electrical resistivity depending on AE. It can be seen from the experimental results that the  $\rho$  values are affected by AE (Si, Bi, Sb, Ni, and Co). It is evident that AE increases the resistivity of Al-Cu based alloy. As shown in Fig. 5a, the addition of Bi and Sb shows the highest values  $7.73 \times 10^{-8} \Omega\text{m}$  and  $7.55 \times 10^{-8} \Omega\text{m}$  of all AE in Al-Cu eutectic, but the lowest  $\rho$  value  $6.99 \times 10^{-8} \Omega\text{m}$  measured from Si addition to Al-Cu under similar growth conditions ( $V \cong 167.08 \mu\text{m s}^{-1}$ ). The reason for these differences, the AE change the electrical resistivity of the Al-Cu because each of them has a different electrical resistivity value at room tem-

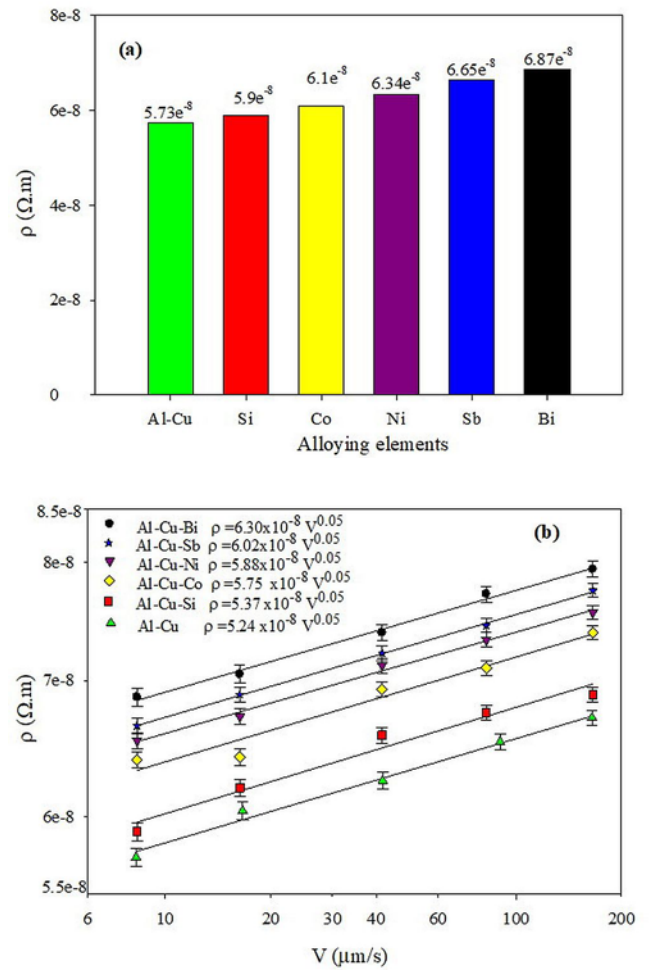


Fig. 5. (a) Variation of electrical resistivity *vs.* alloying elements and (b) variation of electrical resistivity *vs.* solidification rate.

perature. The values of  $\rho$  are (2.75, 1.72, 1.63, 107, 39.0, 7.20, and 6.60)  $\times 10^{-8} \Omega\text{m}$  for pure Al, Cu, Si, Bi, Sb, Ni, and Co, respectively [40]. Since Bi and Sb are semi-metals, their resistivities are very high ( $107 \times 10^{-8}$  and  $39.0 \times 10^{-8} \Omega\text{m}$ , respectively). So, these AE led to a more increase in the resistivity of the Al-Cu eutectic. It can be said that the reason of change of electrical resistivity of Al-Cu is that each AE has a different resistivity value. In addition, alloying elements increase the number of grain boundaries and dislocations in the microstructure. Considering the atomic scale, it can be thought that electrons, which play an important role in the current-conduction process, are exposed to more scattering at the grain boundaries, leading to an increase in resistivity.

The variation of electrical resistivity with the solidification rate ( $V$ ) in the range of 8.28–167.09  $\mu\text{m s}^{-1}$  was measured for Al-Cu-X alloys. The dependence of  $\rho$  values on  $V$  is given in Fig. 5b. As seen in Fig. 5b,

the variation of  $\rho$  as a function of  $V$  can be represented as:

$$\rho = k_5 \times V^e, \quad (5)$$

where  $k_5$  and  $e$  are a constant and an exponent value of  $V$ , respectively.

As shown from Fig. 5b, the values of  $\rho$  increase with the increasing the values of  $V$ . It is found that increase of the values of  $V$  from 8.28 to 167.08  $\mu\text{m s}^{-1}$  leads to an increase in electrical resistivity from  $5.73 \times 10^{-8}$  to  $6.71 \times 10^{-8}$   $\Omega\text{m}$  for Al-Cu based alloys, from  $6.87 \times 10^{-8}$  to  $7.73 \times 10^{-8}$   $\Omega\text{m}$  for Al-Cu-Bi samples. The exponent value of  $d$  is found to be 0.05 for all AE added to Al-Cu, and this value is in good agreement with the values ranging from 0.04 to 0.09 reported by Çadırhet al [28] for Al-Cu-Co, Kaygısız and Maraşlı [29] for Al-Cu-Mg, Kaya et al. [31] for Al-Mn- $x$ Si, and Büyük et al. [32] for Al-Cu-Si-Fe. The reasons for differences in exponent values may be due to the different alloy compositions, microstructural features, and experimental conditions.

#### 4. Conclusions

Based on this study of the effects of alloying elements (Si, Bi, Sb, Ni, and Co) and solidification rates on microstructure, microhardness and ultimate tensile strength and electrical resistivity of Al-33Cu-2X alloys were investigated. As a result of this research, the following conclusions can be drawn:

1. Experimental measurements show that the microstructural features of Al-Cu based alloys varied with AE and solidification conditions. The addition of AE to Al-Cu eutectic and the increased  $V$  values caused the formation of  $\text{Al}_2\text{Cu}$ ,  $\text{Al}_7\text{CoCu}_2$ ,  $\text{Al}_3\text{Ni}$ , and  $\text{AlBi}$  IMC compound phases in the Al-Cu for alloying elements (Co, Ni, and Bi). A higher microhardness and tensile strength were thus achieved.

2. It was found that the addition of AE led to a decrease in lamellar spacings by (11–39) %. Additionally, the increase of the  $V$  values has a significant effect on the microstructure; the empirical relationship between  $\lambda$  and  $V$  is  $\lambda = k_1 \times V^a$ ;  $k_1$  and  $a$  values have minor differences with the AE.

3. Addition of AE caused an increase in HV values of about 6, 16, 12, 8, and 19 % for Si, Bi, Sb, Ni, and Co added to Al-Cu, respectively, for  $V \cong 8.28 \mu\text{m s}^{-1}$ . It was also found that the HV values increase with  $V$ . The relationship between HV and  $V$  can be given as  $\text{HV} = k_2 \times V^b$ ;  $k_2$  and  $b$  values change within the range of values (1659–2138) and (0.03–0.04), respectively, depending on the AE.

4. The relationship between the HV and  $\lambda$  was obtained as  $\text{HV} = k_3 \times \lambda^{-c}$  by linear regression analysis. Depending on AE content, the decreasing lamellar

spacings  $\lambda$  from 3.66 to 0.66  $\mu\text{m}$  increase microhardness values from 1854 to 2604 MPa.

5. Addition of AE led to an increase in UTS values by 10, 32, 29, 19, and 35 % for Si, Bi, Sb, Ni, and Co added to Al-Cu, respectively, for  $V \cong 8.28 \mu\text{m s}^{-1}$ . It was also found that the UTS values increase with the  $V$ . The relationship between UTS and  $V$  can be given as  $\sigma = k_4 \times V^d$ . The values of  $k_4$  and  $d$  change within the range of values (72–107) and (0.11–0.15), respectively, depending on the AE.

6. It was found that the electrical resistivity values change with the AE. While the highest  $\rho$  value ( $7.73 \times 10^{-8}$   $\Omega\text{m}$ ) was measured from the Al-33Cu-2Bi sample, the lowest  $\rho$  value ( $6.89 \times 10^{-8}$   $\Omega\text{m}$ ) was measured from Al-33Cu-2Si alloy (for  $V \cong 167.08 \mu\text{m s}^{-1}$ ). It was also found that the values of  $\rho$  increase with increasing the  $V$  values. From the experimental results, the relationship between  $V$  and  $\rho$  can be written as  $\rho = k_5 \times V^e$ . The values of  $k_5$  and  $e$  vary within the range of values  $(5.24\text{--}6.30) \times 10^{-8}$  and 0.05, respectively.

#### Acknowledgement

This research was supported by Erciyes University Scientific Research Project Unit (FBA 2013–4508).

#### References

- [1] G. E. Totten, D. S. MacKenzie, Handbook of Aluminum. Vol. 2, Alloy Production and Materials Manufacturing, CRC Press, New York, 2003. ISBN 9780824708962
- [2] Metals Handbook Properties and Selection: Non-Ferrous Alloys and Special Purpose Materials, Vol. 2, 10th edition, Metals Park, ASM International, 1990. ISBN-13: 978-0871703781
- [3] F. Ostermann, Anwendungstechnologie Aluminium, 3rd edition, Berlin/Heidelberg, Springer, 2014. ISBN: 978-3-662-43806-0
- [4] S. P. Ravindranathan, K. T. Kashyap, S. Ravi Kumar, C. Ramachandra, B. Chatterji, Effect of delayed aging on mechanical properties of an Al-Cu-Mg alloy, J. Mater. Eng. Perf. 9 (2000) 24–27. [doi:10.1361/105994900770346231](https://doi.org/10.1361/105994900770346231)
- [5] R. Alizadeh, R. Mahmudi, Effect of Sb additions on the microstructural stability and mechanical properties of cast Mg-4Zn alloy, Mat. Sci. Eng. A 527 (2010) 5312–5317. [doi:10.1016/j.msea.2010.05.029](https://doi.org/10.1016/j.msea.2010.05.029)
- [6] M. M. Avedesian, H. Baker (Eds.), ASM Specialty Handbook: Magnesium and Magnesium Alloys, Materials Park, ASM International, 1999. ISBN: 978-0-87170-657-7
- [7] Y. C. Lee, A. K. Dahle, D. H. StJohn, The role of solute in grain refinement of magnesium, Metall. Mater. Trans. A 31 (2000) 2895–2906. [doi:10.1007/BF02830349](https://doi.org/10.1007/BF02830349)

- [8] E. Çadırılı, İ. Yılmaz, M. Şahin, H. Kaya, Investigation of some physical properties of the directionally solidified Al-Cu-Co ternary eutectic alloy, *Trans. Indian Inst. Met.* 68 (2015) 817–827. [doi:10.1007/s11665-020-05253-3](https://doi.org/10.1007/s11665-020-05253-3)
- [9] G. Zhao, J. Chen, C. Ding, M. C. Gu, Y. S. Ye, Influence of the composition on the solidification path, microstructure evolution and mechanical properties of Al-Cu-Mg alloys, *J. Mater. Eng. Perf.* 28 (2019) 6980–6992. [doi:10.1007/s11665-019-04409-0](https://doi.org/10.1007/s11665-019-04409-0)
- [10] N. Charbhai, B. S. Murty, S. Sankaran, Characterization of microstructure and precipitation behavior in Al-4Cu-xTiB<sub>2</sub> in-situ composite, *Trans. Indian Inst. Met.* 64 (2011) 117–121. [doi:10.1007/s12666-011-0023-7](https://doi.org/10.1007/s12666-011-0023-7)
- [11] G. Wang, Q. Sun, L. Shan, Z. Zhao, L. Yan, Influence of indium trace addition on the precipitation behavior in a 357 cast aluminum alloy, *J. Mater. Eng. Perf.* 16 (2007) 752–756. [doi:10.1007/s11665-007-9086-3](https://doi.org/10.1007/s11665-007-9086-3)
- [12] L. Weijing, C. Shihai, H. Jianmin, X. Chao, Effect of silicon on the casting properties of Al-5.0%Cu alloy, *Rare Met.* 25 (2006) 133–135. [doi:10.1016/S1001-0521\(08\)60067-4](https://doi.org/10.1016/S1001-0521(08)60067-4)
- [13] V. Zakharov, Effect of scandium on the structure and properties of aluminum alloys, *Metal. Sci. Heat Treat.* 45 (2003) 246–253. [doi:10.1023/A:1027368032062](https://doi.org/10.1023/A:1027368032062)
- [14] S. Hirose, T. Sato, A. Kamio, H. Flower, Classification of the role of microalloying elements in phase decomposition of Al based alloys, *Acta Mater.* 48 (2000) 1797–1806. [doi:10.1016/S1359-6454\(99\)00475-9](https://doi.org/10.1016/S1359-6454(99)00475-9)
- [15] P. N. Raju, K. S. Rao, G. Reddy, M. Kamaraj, K. P. Rao, Microstructure and high temperature stability of age hardenable AA2219 aluminium alloy modified by Sc, Mg and Zr additions, *Mater. Sci. Eng. A* 464 (2007) 192–201. [doi:10.1016/j.msea.2007.01.144](https://doi.org/10.1016/j.msea.2007.01.144)
- [16] K. Yu, W. Li, S. Li, J. Zhao, Mechanical properties and microstructure of aluminum alloy 2618 with Al<sub>3</sub>(Sc, Zr) phases, *Mater. Sci. Eng. A* 368 (2004) 88–93. [doi:10.1016/j.msea.2003.09.092](https://doi.org/10.1016/j.msea.2003.09.092)
- [17] S. Banerjee, P. Robi, A. Srinivasan, P. K. Lakavath, Effect of trace additions of Sn on microstructure and mechanical properties of Al-Cu-Mg alloys, *Mater. Des.* 31 (2010) 4007–4015. [doi:10.1016/j.matdes.2010.03.012](https://doi.org/10.1016/j.matdes.2010.03.012)
- [18] H. Kamali, M. Emamy, A. Razaghian, The influence of Ti on the microstructure and tensile properties of cast Al-4.5Cu-0.3Mg alloy, *Mater. Sci. Eng. A* 590 (2014) 161–167. [doi:10.1016/j.msea.2013.10.032](https://doi.org/10.1016/j.msea.2013.10.032)
- [19] S. Banerjee, P. Robi, A. Srinivasan, L. P. Kumar, High temperature deformation behavior of Al-Cu-Mg alloys micro-alloyed with Sn, *Mater. Sci. Eng. A* 527 (2010) 2498–2503. [doi:10.1016/j.msea.2010.01.052](https://doi.org/10.1016/j.msea.2010.01.052)
- [20] S. A. Salihu, A. Isah, P. Evarastics, Influence of magnesium addition on mechanical properties and microstructure of Al-Cu-Mg alloy, *IOSR J. Pharm. Biol. Sci.* 4 (2012) 15–20. [doi:10.9790/3008-0451520](https://doi.org/10.9790/3008-0451520)
- [21] R. Z. Valiev, M. Yu. Murashkin, I. Sabirov, A nanos- tructural design to produce high-strength Al alloys with enhanced electrical conductivity, *Scripta Mater.* 76 (2014) 13–16. [doi:10.1016/j.scriptamat.2013.12.002](https://doi.org/10.1016/j.scriptamat.2013.12.002)
- [22] G. I. Meshchanov, I. B. Peshkov, Innovative ap- proaches in domestic cable engineering, *Russ. Electr. Eng.* 81 (2010) 1–8. <https://doi.org/10.3103/s1068371210010013>
- [23] D. J. Hagmaier, Evaluation of heat damage to alu- minium aircraft structures, *Mater. Eval.* 40 (1982) 942–969.
- [24] R. Z. Valiev, M. Y. Murashkin, A. V. Ganeev, N. A. Enikeev, Superstrength of nanostructured met- als and alloys produced by severe plastic deforma- tion, *Phys. Met. Metallogr.* 113 (2012) 1193–1201. [doi:10.1134/S0031918X12130042](https://doi.org/10.1134/S0031918X12130042)
- [25] H. S. Abdo, A. H. Seikh, J. A. Mohammed, M. S. Soliman, Alloying elements effects on electri- cal conductivity and mechanical properties of newly fabricated Al based alloys produced by conven- tional casting process, *Materials* 14 (2021) 3971–3981. [doi.org/10.3390/ma14143971](https://doi.org/10.3390/ma14143971)
- [26] A. Aker, H. Kaya, Measurements of electrical and thermal properties with growth rate, alloying elements and temperature in the Al-Si-X alloys, *I. J. Cast Met- als Res.*, 30 (2017) 293–300. [doi.org/10.1080/13640461.2017.1307623](https://doi.org/10.1080/13640461.2017.1307623)
- [27] H. Kaya, A. Aker, Effect of alloying elements and growth rates on microstructure and mechanical prop- erties in the directionally solidified Al-Si-X alloys, *J. Alloys Comp.* 694 (2017) 145–154. [doi:10.1016/j.jallcom.2016.09.199](https://doi.org/10.1016/j.jallcom.2016.09.199)
- [28] E. Çadırılı, A. Aker, Y. Kaygısız, M. Şahin, Influences of growth velocity and Fe content on microstructure, microhardness and tensile properties of directionally solidified Al-1.9Mn-xFe ternary alloys, *Mater. Res.* 20 (2017) 801–813. [doi:10.1590/1980-5373-MR-2017-0048](https://doi.org/10.1590/1980-5373-MR-2017-0048)
- [29] Y. Kaygısız, N. Maraşlı, Microstructural, mechanical, and electrical characterization of directionally solidi- fied Al-Cu-Mg eutectic alloy, *Physics Metals Metall.* 118 (2017) 389–398. [doi:10.1134/S0031918X17040123](https://doi.org/10.1134/S0031918X17040123)
- [30] U. Büyük, S. Engin, H. Kaya, E. Çadırılı, N. Maraşlı, Directionally solidified Al-Cu-Si-Fe quaternary eutec- tic alloys, *Phys. Metals Metall.* 121 (2020) 78–83. <https://doi.org/10.1134/S0031918X20010044>
- [31] H. Kaya, E. Çadırılı, U. Büyük, Microstructure, micro- hardness, tensile, electrical, and thermal properties of the Al-Mn-xSi ternary alloys, *Kovove Mater.* 58 (2020) 275–285. [http://doi.org/10.4149/km\\_2020\\_4\\_275](http://doi.org/10.4149/km_2020_4_275)
- [32] J. Lapin, J. Marecek, Effect of growth rate on microstructure and mechanical properties of direc- tionally solidified multiphase intermetallic Ni-Al-Cr- Ta-Mo-Zr alloy, *Intermetallics* 14 (2006) 1339–1344. [doi:10.1016/j.intermet.2005.10.016](https://doi.org/10.1016/j.intermet.2005.10.016)
- [33] J. Fan, X. Li, Y. Su, R. Chen, J. Gou, H. Fu, Depen- dency of microstructure parameters and microhard- ness on the temperature gradient for directionally so- lidified Ti-49Al alloy, *Mater. Chem. Phys.* 130 (2011) 1232–1238. [doi:10.1016/j.matchemphys.2011.09.002](https://doi.org/10.1016/j.matchemphys.2011.09.002)
- [34] J. Fan, X. Li, Y. Su, J. Guo, H. Fu, Dependency of microhardness on solidification processing parameters and microstructure characteristics in the directionally solidified Ti-46Al-0.5W-0.5Si alloy, *J. Alloys Comp.* 504 (2010) 60–64. [doi:10.1016/j.jallcom.2010.05.095](https://doi.org/10.1016/j.jallcom.2010.05.095)
- [35] J. Lapin, L. Ondruš, M. Nazmy, Directional solidi- fication of intermetallic Ti-46Al-2W-0.5Si alloy in alumina moulds, *Intermetallics* 10 (2002) 1019–1031. [doi:10.1016/S0966-9795\(02\)00119-X](https://doi.org/10.1016/S0966-9795(02)00119-X)
- [36] J. Lapin, Z. Gabalcová, O. Bajana, The effect of mi- crostructure on mechanical properties of direc- tionally solidified intermetallic Ti-46Al-8Nb alloy, *Kovove Mater.* 47 (2009) 159–167.

- [37] ASTM E8/E8M-13a, Standard Test Methods for Tension Testing of Metallic Materials, ASTM International, West Conshohocken, PA, 2013.  
[doi: 10.1520/E0008\\_E0008M-13A](https://doi.org/10.1520/E0008_E0008M-13A)
- [38] F. M. Smiths, Measurement of sheet resistivities with the four-point probe, Bell Syst. Tech. J. 37 (1958) 711–718. [doi:10.1002/j.1538-7305.1958.tb03883.x](https://doi.org/10.1002/j.1538-7305.1958.tb03883.x)
- [39] J. De Wilde, L. Froyen, S. Rex, Coupled two-phase  $[\alpha(\text{Al})+\theta(\text{Al}_2\text{Cu})]$  planar growth and destabilization along the univariant eutectic reaction in Al-Cu-Ag alloys, Scripta Mater. 51 (2004) 533–538. [doi:10.1016/j.scriptamat.2004.05.040](https://doi.org/10.1016/j.scriptamat.2004.05.040)
- [40] K. A. Jackson, J. D. Hunt, Lamellar and rod eutectic growth, Trans. Met. Soc. AIME 236 (1966) 1129–1141.
- [41] Jerry C. Whitaker (Ed.), The Electronics Handbook, Technical Press Inc., Boca Raton, CRC Press, 1996. ISBN 9780849318894